

Observation of vortices and field correlations in the near-field speckle of a three-dimensional photonic crystal

Silvia Vignolini,^{1,*} Matteo Burresti,^{2,1} Stefano Gottardo,¹ L. Kuipers,² and Diederik S. Wiersma¹

¹LENS and National Institute for Optics (CNR-INO), IT-50019 Sesto Fiorentino Firenze, Italy

²Center for Nanophotonics, FOM Institute for Atomic and Molecular Physics (AMOLF),
Science Park 113, 1098 XG Amsterdam, The Netherlands

*Corresponding author: vignolini@lens.unifi.it

Received February 22, 2010; revised April 20, 2010; accepted May 16, 2010;
posted May 18, 2010 (Doc. ID 124454); published June 8, 2010

We present a phase-sensitive near-field study of speckle fields from photonic crystals in the presence of disorder. We observe phase singularities (vortices) and analyze their statistical properties and screening effects. The experimental results show a clear polarization dependence, not only in their morphological parameters but also in their spatial distribution. © 2010 Optical Society of America

OCIS codes: 160.5298, 180.4243, 260.6042.

Phase singularities are lines in space or points in a plane where the phase of a complex scalar wave is undefined and the amplitude is zero. In the neighborhood of such singularities, the gradient of the phase changes quickly through all of its values. Phase singularities for sound waves were observed already in 1973 [1] and were later studied for several other wave phenomena [2], including radio, microwaves [3], and optical waves [4,5]. The positions of such phase singularities and their morphological properties are not independent; they are strongly correlated to the optical properties of the dielectric material under study [6,7]. Consequently, singular optics has received much interest in the photonic community [8,9]. The statistical properties of a speckle pattern are a clear fingerprint of the multiple scattering that occurs in the sample, as intensively shown in near-field investigation at the microwave regime [10–12]. From such information, however, it is also possible to characterize the optical properties of real ordered structures, which are inevitably affected by structural disorder [13].

Here, we report on a near-field investigation, at optical frequencies, of speckle patterns and phase singularities generated by a three-dimensional photonic crystal with a significant degree of disorder. We experimentally demonstrate the near-field polarization dependence of the vortex field by studying both the vortices morphological parameters and their screening effect. Comparison of experimental results with theory for isotropic random field show similarities as well as differences, emphasizing the role of the disorder and polarization on the studied system.

The sample under investigation is a silica synthetic opal grown using a dip-coating technique [14]. The microspheres that constitute the photonic structure have a diameter of 730 nm. Far-field reflection measurements, performed along the $\Gamma - L$ direction of the opal, exhibit a Bragg peak centered at 1550 nm with a reflectivity of roughly 30%. This relatively low value of reflectivity indicates that the studied opal has an appreciable degree of disorder. We perform a set of measurements in the same zone of the sample for different incident wavelengths ranging from 1440 nm to 1590 nm using a scanning near-field

microscope (SNOM) combined with a Mach–Zehnder type interferometer [5,9]. Linearly polarized laser light is coupled into the structure by focusing it at one side of the (111) plane of the opal; see Fig. 1(a). An aluminum-coated tapered fiber with a subwavelength aperture (near-field probe) is kept at an ~ 20 nm distance from the sample. A minute fraction of the evanescent field of the light transmitted through the sample is coupled to the probe and detected. By combining the near-field microscope with an interferometer, we are able to probe the amplitude and the phase distributions with subwavelength resolution, allowing us to reconstruct the field as

$$E(\mathbf{r}) = A(\mathbf{r}) \exp i\varphi(\mathbf{r}) = f_{\text{Re}}(\mathbf{r}) + if_{\text{Im}}(\mathbf{r}), \quad (1)$$

where $\mathbf{r} = (x, y)$, A and φ indicate the amplitude and the phase of the optical field, and f_{Re} and f_{Im} are its real and imaginary parts, respectively.

Figure 1(b) shows a typical map of the electric field amplitude A collected by the near-field probe outside at $\lambda = 1442$ nm, where the speckle fluctuations are clearly recognizable. The map of the electric field amplitude in Fig. 1(b) is compared with the map of the phase in Fig. 1(c). Phase singularities [black dots in (c)] correspond to zero amplitude [white dots in (b)]. To locate the position of the singularities accurately, we identify the lines where f_{Re} (gray lines) and f_{Im} (black line) are zero, respectively. The vortex centers are then located at the crossing points of these lines (because both the real and the imaginary part have to be zero at the singularity; see Fig. 1(d)). The vortex positions are indicated by the full and empty dots at intersections between the gray and black lines. In the case of speckle pattern generated from a complete random system and in the far-field region, the vortices must obey a fundamental sign principle [6]. This means that, when a certain vortex has an increasing phase when rotating clockwise, its adjacent should have a decreasing phase when rotating in the same direction. The reason behind this concept is topological, and should therefore hold for any type of vortex field, including the ones generated by a partially disordered photonic crystal. We verify the sign principle for the vortices observed in our sample

by calculating along the two directions in the plane, the derivatives of the phase at the position of the vortices. Figure 1(d) shows that the nearest neighbors vortices are also anticorrelated for the speckle field generated in the near-field region. The sign of the vortices is strictly related to their spatial distribution as well. To obtain a more quantitative understating of the vortex screening, we can calculate, from the experimental data, the charge correlation function (C_Q) [15] as

$$C_Q(\Delta\mathbf{r}) = \frac{2}{\eta} \langle N_+(0)[N_+(\Delta\mathbf{r}) - N_-(\Delta\mathbf{r})] \rangle - \delta(\Delta\mathbf{r}), \quad (2)$$

where $N_{+/-}(\Delta\mathbf{r})$ is the number density of positive/negative vortices at position \mathbf{r} , η is the total number of vortices ($N \simeq 2N_+ \simeq 2N_-$), and the Dirac delta function δ takes into account the fact that the charge at the origin is correlated with itself. The spatial distribution of the in-

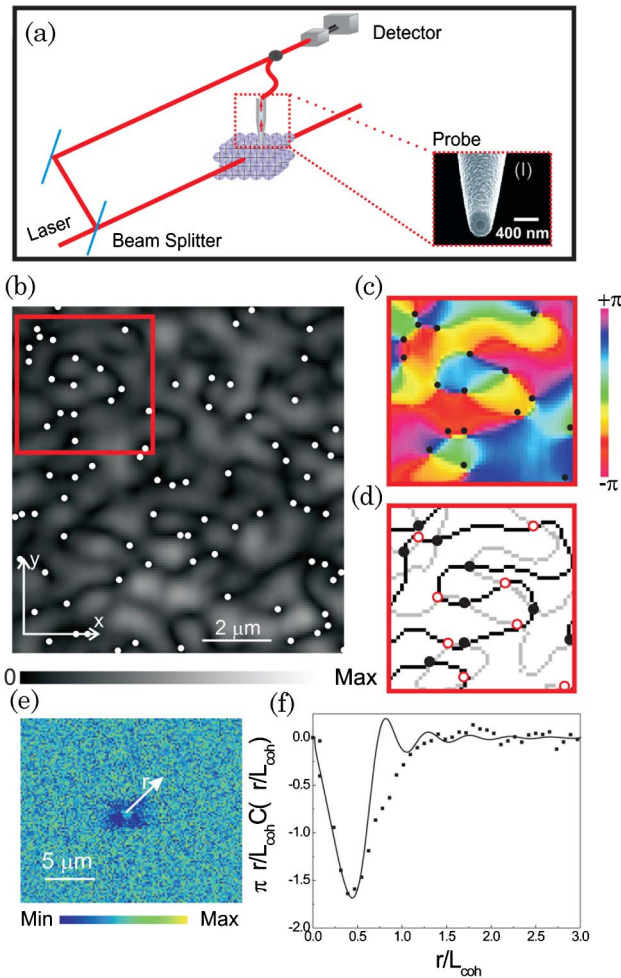


Fig. 1. (Color online) (a) Schematic representation of the setup. The inset (I) shows a scanning electron microscope image of the near-field probe. (b) Example of the electric field amplitude distribution collected by the near-field microscope at $\lambda = 1442$ nm. The white dots in correspondence of the zero values of the field amplitude correspond to vortice positions. (c), (d) Phase map and the map of the zero lines of the real part and the imaginary part of the field are presented, respectively, in correspondence to region indicated by the square in (a). (e) Map of the integrated charge correlation function C_Q obtained from the experiential data. (f) Angular average of $C_Q(\Delta\mathbf{r})$ compared with the calculated expression.

tegrated charge correlation function is shown in Fig. 1(e). The points in Fig. 1(f) represent the averaged radial profile of C_Q . It is interesting to notice that C_Q is mostly negative as expected in the case of screening. By comparing this curve with the theoretical expression given in [15], we find a coherence value of $1.5 \mu\text{m}$.

We calculate from the experimental data the vortex morphological parameters and their statistical probability densities [1,2,4,6]. In particular, we investigate the statistical behavior of the geometrical parameters associated to the tangent planes of f_{Re} and f_{Im} at the vortex position as defined in [16]. Figure 2(a) provides a schematic representation of these parameters. We define ρ_{Re} and ρ_{Im} as the angles between the normal of the tangent planes and the x axis, and $\tan \phi_{\text{Re}}$ and $\tan \phi_{\text{Im}}$ are their slopes. In Fig. 2(b), the angular distribution ρ_{Re} is presented. This distribution shows two well-defined maxima in correspondence of $\pm(\pi/2)$. For the angular distribution of ρ_{Im} , which is not reported here, the same behavior is obtained. The fact that the vortices are predominantly oriented along the y axis (that is, perpendicular with respect the polarization direction) can again be attributed to the polarization dependence of the speckle pattern in the near field [17,18]. In Fig. 2(c) the probability distribution of the vortex anisotropy ($\alpha = (\tan \phi_{\text{Im}} / \tan \phi_{\text{Re}})$) is reported. In the histogram, the bin that contains most counts is $\alpha = 0.75$, indicating that in most cases the vortices present a certain degree of anisotropy. Finally, Fig. 2(d) shows the probability distribution of the vortex amplitude $a = \tan \phi_{\text{Re}}$. This probability is analogous to the one calculated for the isotropic random case.

To obtain a deeper insight of the role of the disorder in our system, we retrieve from our data the spectral correlation function. Figures 3(a) and 3(b) show the real part of the spatial correlation function obtained from the measurements, outside and inside the pseudo-gap region, respectively. In both figures, we observe an evident radial anisotropy that is explained considering the polarization dependence of the near-field speckle pattern [17,18]. In both cases, the spatial correlation length of

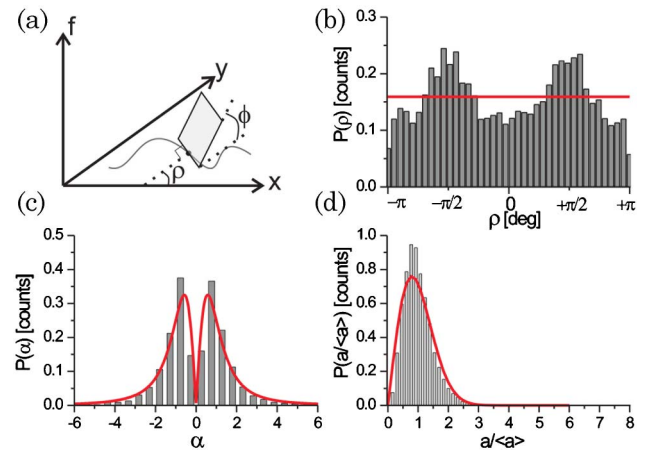


Fig. 2. (Color online) (a) Schematic representation of the geometry of the real/imaginary tangent plane: the angle that measures the orientation of the plane with respect to the x axes is ρ , while the slope of the plane is ϕ . (b)–(d) Vortex morphological parameters distributions for ρ , α , and a , respectively. The red curves in the graphs represent the expected behavior for such parameters for the isotropic random field case.

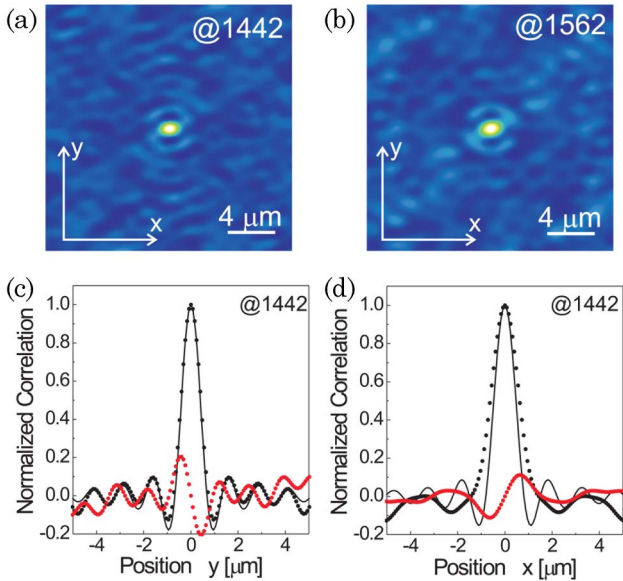


Fig. 3. (Color online) (a), (b) Real part of the spatial correlation function of the electric field for $\lambda = 1442$ nm and $\lambda = 1562$ nm, respectively. (c) The dotted black line in the graph reports the cut along the y direction of the real part of the spatial correlation function, while the dotted red (gray) line reports the imaginary part. The black straight line is the fit of the real part of the correlation function obtained considering the theory for random systems reported in [11]. (d) Same as (c) for the x direction. The black straight line is the expression of the real part of the correlation function considering a refractive index equal to 1.

the field is significantly larger in the direction of the polarization (along the x axis) than in the perpendicular direction. This observation indicates that the effect is not related to the photonic crystal structure because its optical property are strongly wavelength dependent. By comparing our experimental results to the complete isotropic random case [11] we observe that the spatial correlation profile along the y direction corresponds well to the theoretical curve for a completely disordered system. From the comparison, it is possible to estimate the effective refractive index [see Fig. 3(c)], which gives $n = 1.07 \pm 0.07$, and the coherence length that is agreement with the value estimated from the C_Q . These values are constant within the error for all the wavelengths considered. The spatial correlation profile taken along the x direction has a different shape, which cannot be fitted with the same expression [see Fig. 3(d)]. In this case, to match the width of the central peak, one would obtain a refractive index value smaller than 1. These observation clearly indicate polarization dependencies of the speckle pattern generated by the investigated sample. The anisotropy in the field correlation shows that the polarization is not completely randomized during the multiple scattering processes, as predicted in [17,18] and observed in [19]. The red (gray) dotted curves in Figs. 3(c) and 3(d) are the profile along the y direction of the imaginary part

of the spatial correlation function. We can clearly recognize that the imaginary part exhibits oscillations, above the noise level. This interesting behavior is absent in regular disordered structures, because the imaginary part of $C_E(\Delta\mathbf{r})$ vanishes for homogeneous isotropic structures [11]. These oscillations, therefore, suggest the presence of the underlying photonic crystal structure.

In conclusion, we studied the near-field speckle of three-dimensional photonic crystals. We observed vortices and analyzed their morphological parameters. Our work shows that a phase-sensitive near-field investigation reveals the influence of disorder on light propagation in photonic crystals.

We wish to thank B. Shapiro, K. Vynck, F. Intonti, L. Bacci, and R. Sapienza for fruitful discussions. This work is part of the research program of the Stichting voor Fundamenteel Onderzoek der Materie (FOM), which is financially supported by the Nederlandse organisatie voor Wetenschappelijk Onderzoek (NWO). Support by the NWO (VICI grant) is gratefully acknowledged. This work is also supported by the European Network of Excellence Nanophotonics for energy efficiency.

References

1. J. F. Nye and M. V. Berry, Proc. R. Soc. A **336**, 165 (1974).
2. M. V. Berry and M. R. Dennis, Proc. R. Soc. A **456**, 2059 (2000).
3. S. Zhang and A. Z. Genack, Phys. Rev. Lett. **99**, 203901 (2007).
4. W. Wang, S. G. Hanson, Y. Miyamoto, and M. Takeda, Phys. Rev. Lett. **94**, 103902 (2005).
5. M. L. M. Balistreri, J. P. Korterik, L. Kuipers, and N. F. van Hulst, Phys. Rev. Lett. **85**, 294 (2000).
6. N. Shvartsman and I. Freund, Phys. Rev. Lett. **72**, 1008 (1994).
7. M. R. Dennis, Proc. SPIE **4403**, 13 (2001).
8. M. R. Dennis, R. P. King, B. Jack, K. O'Holleran, and M. J. Padgett, Nature Phys. **6**, 118 (2010).
9. M. Buresi, R. J. P. Engelen, A. Opheij, D. van Oosten, D. Mori, T. Baba, and L. Kuipers, Phys. Rev. Lett. **102**, 033902 (2009).
10. B. Shapiro, Phys. Rev. Lett. **57**, 2168 (1986).
11. P. Sebbah, R. Pnini, and A. Z. Genack, Phys. Rev. E **62**, 7348 (2000).
12. P. Sebbah, B. Hu, A. Z. Genack, R. Pnini, and B. Shapiro, Phys. Rev. Lett. **88**, 123901 (2002).
13. V. M. Apalkov, M. E. Raikh, and B. Shapiro, Phys. Rev. Lett. **92**, 253902 (2004).
14. P. Jiang, J. F. Bertone, K. S. Hwang, and V. L. Colvin, Chem. Mater. **11**, 2132 (1999).
15. B. I. Halperin, in *Physics of Defects* (North Holland, 1981).
16. I. Freund, J. Opt. Soc. Am. A **11**, 1644 (1994).
17. A. Apostol and A. Dogariu, Phys. Rev. Lett. **91**, 093901 (2003).
18. C. Liu and S.-H. Park, Opt. Lett. **30**, 1602 (2005).
19. V. Emiliani, F. Intonti, M. Cazayous, D. S. Wiersma, M. Colocci, F. Aliev, and A. Lagendijk, Phys. Rev. Lett. **90**, 250801 (2003).